Microfluidic droplet control by photothermal interfacial flow

Masakazu MUTO [1,*], Masahiro MOTOSUKE [1,2]

* Corresponding author: Tel.: +81 (3)58761717; Fax: +81 (3)58761326; Email: j4513652@ed.tus.ac.jp
1 Department of Mechanical Engineering, Tokyo University of Science, Japan
2 Research Institute for Science and Technology, Tokyo University of Science, Japan

Abstract Droplet-based microfluidics is an emerging field that can perform a variety of discrete operation of tiny amount of reagent or individual cell. Noncontact manipulation of droplets in a microfluidic platform can be achieved by using the Marangoni convection due to a local temperature gradient given by the irradiation of heating light. This method provides noncontact, selective and flexible manipulation for droplets flowing in microfluidic network. Although the potential of this selective operation method of droplets was confirmed, the driving force exerted on droplets has not been quantitatively obtained. In this study, we have developed a measurement system of the temperature field around droplets during the manipulation by light irradiation and evaluated the manipulation force. In O/W emulsion system with oleic acid and buffer solution, oleic acid for droplet and buffer solution for continuous phase, the temperature distribution around the droplets was measured by laser-induced fluorescence. From the balance of drag force and photo-induced Marangoni force, the driving force was determined. From the results, we confirmed the applicability of the noncontact droplet manipulation using the photothermal Marangoni effect.

Keywords: Microfluidics, Droplet, Photothermal Marangoni Effect, Laser-Induced Fluorescence

1. Introduction

Recently, there has been a growing interest in the microfluidic technology due to the highly diverse applications from point-of-care diagnostics to microreactors. An approach using multiphase flow, so-called droplet-based microfluidics, focuses on creating and controlling discrete volumes involving cells and reagents in the dispersed phase. Since the effects of interfacial phenomena become dominant with decrease of the length scale in microfluidic devices, local control of interfacial tension can be effective for droplet manipulation.

Normally, pathway of droplet in a microdevice is determined by the channel geometry (The et al, 2008). We have proposed a remote manipulation technique of droplets in a microfluidic platform by using the Marangoni convection due to a local temperature gradient given by the light irradiation (Muto et al, 2013). The concept of the droplet manipulation system is shown in Fig. 1. When the heating light is irradiated into the liquid in the vicinity of a droplet, it generates the Marangoni convection owing to the gradient of temperature-sensitive interfacial tension and results in a pressure difference around the droplet. Then a driving force works on the droplet and moves it toward an area with lower pressure, that is, lower interfacial tension. The liquid-liquid interface in the present study has positive temperature dependence of the tension, and this means the droplet moves away from the heating light position. In our method, the temperature gradient is generated by the light irradiation so that the heating pattern can be easily controlled.

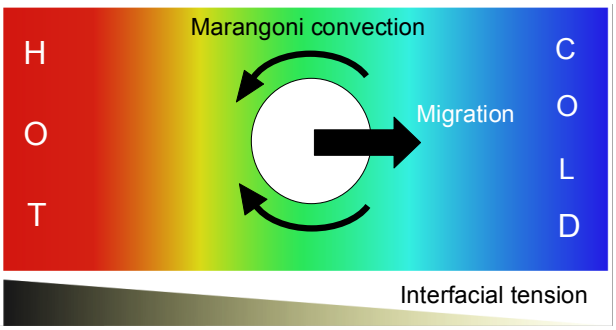

Figure 1: Schematic of droplet migration by Marangoni effect under positive temperature dependence of interfacial tension ($\partial\sigma/\partial T > 0$)

Although this droplet manipulation method provides noncontact, selective and flexible manipulation for droplets flowing in a microchannel network, the driving force exerted on droplets has not been quantitatively obtained. Baroud et al. (2007) had estimated the manipulation force induced by the photothermally actuated Marangoni convection using a focused laser from flow resistance generated by the trapped droplet, however, this method was available only in a specific size of the droplet and microchannel. In this study, we proposed an evaluation of the manipulation force exerted on the droplet based on the measurement of the temperature distribution around the droplets with laser-induced fluorescence (LIF). This method provides the temperature field of liquid in a microfluidic channel which would be useful to evaluate the force field for droplets under an arbitrary shaped light irradiation by a projector or a photomask. From the balance of drag force and photo-induced Marangoni force, the driving force was determined using the measured temperature gradient of the droplet.

2. Experimental System

2.1 Heating optical setup and measurement setup

Fig. 2(a) shows a schematic of the heating optical system to induce a local interfacial tension gradient around a droplet in a microfluidic device by a reduced-projection exposure optics. As for the reduced-projection system, a laser light is irradiated into liquid in a fluidic channel after forming an irradiation pattern characterized by a photomask and reducing the size by optics. The optical system of the reduced-projection was built in an inverted microscope to achieve a co-axial illumination, in which the illumination and the observation optical path had the same axis. The heating optical system consists of a light source (laser), a beam expander (BE), and an imaging lens (IL). The light from the red diode laser with the wavelength of 635 nm was expanded by the beam expander and was passed an imaging lens, and was irradiated into the device. The observation system consists of a sCMOS camera (1920 × 1440 pixels), a filter cube and a mercury lump. A dichroic mirror 1 (DCM 1) was designed to pass the heating laser beam and fluorescence to perform laser-induced fluorescence (LIF) measurement and to reflect the excitation wavelength for the fluorescent dye. A dichroic mirror 2 (DCM 2) was designed to pass the fluorescence and to reflect the heating laser beam. An objective lens (Obj) used in the present study has a magnification of 20 and NA of 0.45.

2.2 Microfluidic device

Fig. 2(b) shows a sectional view of the microfluidic devices. The device consists of two PDMS (polydimethylsiloxane) channel layers. The PDMS channels were fabricated by the standard softlithography (Xia and Whitesides, 1998) using reverse mold of SU-8 on silicone substrate. In order to prevent adhesion of droplet to the channel wall, the PDMS surface was treated to be hydrophilic by a plasma processor. A glass slide made of borosilicate glass was sandwiched between the two PDMS sheets. Droplets were seeded from a bottom channel to a top layer which has a junction and observation area downstream. This two-layer injection system of droplets was employed to ensure the stable seeding of droplets into the observation channel. The channel width of the bottom layer was 200 μm. The top view of the device is shown in Fig. 2(c). The device has two inlets; inlet A is for O/W emulsion and inlet B is for sheath flow of a buffer solution. The sheath flow was used to control the speed of flowing droplet suitable for the manipulation and measurement. The irradiation of the heating light was carried out 1000 μm downstream of the junction. All the inlets were connected to separate syringe pumps. Channel widths of droplet inlet, sheath flow and observation were 100, 200 and 500 μm, respectively. The height of the channel was set at 50 μm in both fluidic channel layers. These dimensions were employed to obtain the irradiated light pattern to heat the liquid without height dependence, which resulted in a physically simple temperature field, namely two-dimensional one. The device was placed on two Peltier elements that were connected to

a water-circulated heat sink controlled by a thermostat. An adhesive thermo-conductive sheet was used to reduce thermal resistance between the device and the Peltier elements. A K-type thermocouple with a thickness of 40μm was attached near the microchannel to obtain the reference temperature of the device used in a calibration procedure of LIF.

2.3 Droplet system

In our experiments, O/W emulsion system was employed; tetraborate buffer solution for the continuous phase (surrounding fluid) and oleic acid for the dispersed phase (droplet). Since both liquids does not absorb light with a wavelength of 635 nm, a small amount of dye substance was added only in the continuous phase to enhance the absorption of the illuminated light. In this study, 1.0 mM Brilliant Blue FCF ($C_{37}H_{34}N_2O_9S_3$) was used as the absorption dye. Additionally, in order to measure the temperature distribution around the droplets by LIF, a temperature-sensitive fluorescent dye, fluorescein, ($C_{20}H_{12}O_5$) with the concentration of 5.0 mM was added into the buffer solution. Depending on fluorescence dye types, pH change would affect the fluorescent intensity. Fluorescein used in this study has strong pH dependence on the fluorescent intensity as well as the temperature. Thus, the buffer solution was used to maintain pH at 9.18 (at 25 degC). Also, 10.0 mM Tween 20 ($C_{18}H_{34}O_6$) was added as a surfactant to stabilize the droplet. The O/W emulsion was generated with a stirrer (1500 rpm, 20s). The droplet size ranged from 10 to 50 μm in diameter, namely 5 to 65 pL in volume.

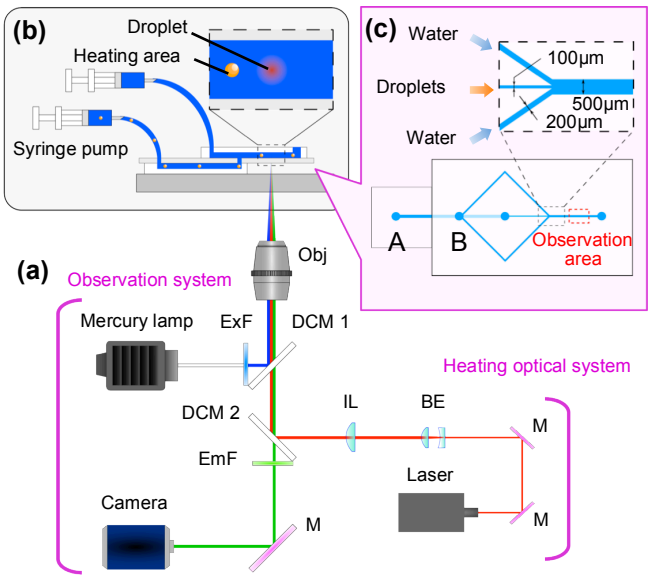

Figure 2: Schematic diagram of (a) heating and measurement optical setup, (b) sectional view of microfluidic device, and (c) top view of the device

3. Results and Discussion

3.1 Establishment of temperature-measurement system with laser-induced fluorescence

When measuring the temperature distribution around the droplets with the laser heating by LIF, the calibration curve between the liquid temperature and the fluorescent intensity is needed in advance. Since the accuracy of the temperature measurement by LIF is determined by the calibration, it is essential to secure precise calibration process. The fluorescent intensity was obtained in a temperature range from 20 to 60 degC both in heating and cooling processes to confirm no hysteresis. The fluorescent intensity in the calibration process was obtained by the mean value on central 200 × 200 pixels over 20 images successively recorded at 22 ms intervals. To prevent quenching of fluorescence during the calibration process, the fluid was seeded with a syringe pump. We also recorded 20 images without the laser heating for the background image to remove the inherent noise due to dark current noise or strayed light.

From the above, we obtained the optimized calibration curve that a surfactant and an absorbing dye were added into the buffer solution with the fluorescence dye as shown in Fig. 3. The calibration function which related the fluorescence to the liquid temperature was determined using a cubic polynomial fitting. The fluorescent intensity showed negative temperature dependence as in the figure; approximately -0.87 %/K at 40 degC. It was confirmed that the surfactant concentration had no influence on the fluorescent intensity.

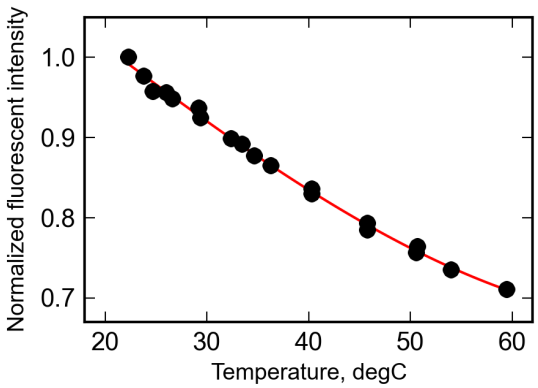

Figure 3: Calibration curve

3.2 Droplet manipulation by laser heating

3.2.1 Temperature distribution during droplet manipulation

An overlapped raw image (960 × 720 pixels) of a droplet manipulated by the laser heating is shown in Fig. 5 (a). In this experimental condition, the laser power was 250 mW and the flow rates of the continuous and dispersed phases were 100 and 30 µl/hr, respectively. The frame rate was 10 fps. In the LIF measurement, the background image was taken without the droplet and the laser heating, and the intensity ratio of each pixel was obtained by dividing the intensity with the droplet and the laser heating by one of the background image. The measured temperature field measured by LIF is shown in Fig. 5 (b). Here, the laser heating raised the temperature of the fluid up to around 60 degC. We recognized that droplets flowed downstream avoiding the heated area. This motion was attributed to the photothermal Marangoni effect. Under the laser heated temperature gradient around the droplet, the interfacial flow occurs due to the thermally-induced tension gradient, and it generates the manipulation force on the droplet toward the cold area. Additionally, there was no significant distortion in the temperature profile when the droplet passed near the heated area. This means that there is no influence of the Marangoni convection generated at the liquid-liquid interface of the droplet which would affect the temperature field due to low Peclet number in the system.

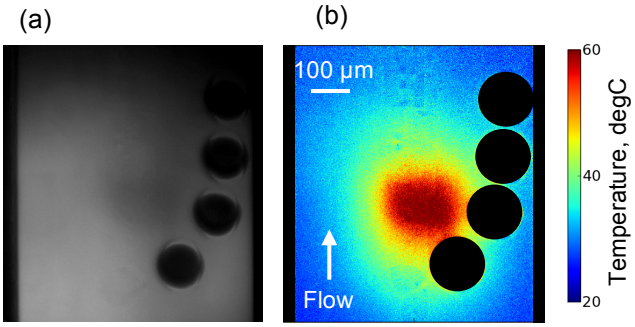

Figure 5: (a) Snapshots of controlled droplet during manipulation and (b) converted temperature distribution

3.2.2 Effect of droplet size on manipulation performance

Difference in trajectories of droplets with different sizes from approximately 20 to 80 µm under the same laser irradiation of 200 mW is depicted in Fig. 6. Each plot presents the center of the droplet with the time interval of 50 ms. This result clearly shows that larger droplet has increased transportation distance from the heated area. In the same temperature gradient, a large temperature difference is generated at both ends of large droplet so that a strong driving force by Marangoni convection is produced on the liquid-liquid interface. Therefore, the driving force of droplet depends on the droplet size and the temperature gradient.

3.3 Evaluation of manipulation force

The manipulation force of a droplet by the photothermal Marangoni convection was quantitatively evaluated. Droplet migration velocity U_M, by Marangoni convection under

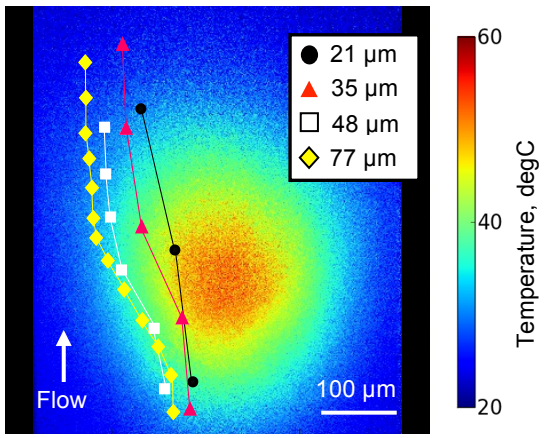

Figure 6: Trajectory of droplets with different sizes

uniform temperature gradient was calculated by Young et al (1959) presented as,

$$U_M = \frac{d\lambda_c(\partial\sigma/\partial T)(\partial T/\partial x)}{(2\eta_c + 3\eta_d)(2\lambda_c + \lambda_d)} \quad (1)$$

where d the droplet diameter, λ the thermal conductivity, $\partial\sigma/\partial T$ the temperature-dependent interfacial tension, $\partial T/\partial x$ the uniform temperature gradient, subscript c and d the continuous phase and dispersed phase. The manipulation force on the droplet F_M can be presented by corrected Hadamard-Rybczynski equation as in Eq. (2).

$$F_M = \pi\eta_c d U_M \left(\frac{2\eta_c + 3\eta_d}{\eta_c + \eta_d}\right)\kappa \quad (2)$$

where η the viscosity of the fluid, κ the wall correction factor as a function of blockage ratio d/h (Chen et al, 1991). In this study, $\partial T/\partial x$ was converted to ΔT, temperature difference between both sides of the droplet measured by LIF, with an assumption of $\partial T/\partial x = \Delta T/d$. Consequently, the force can be presented in Eq. (3).

$$F_M = \frac{\pi\eta_c\lambda_c\kappa(\partial\sigma/\partial T)}{(\eta_c + \eta_d)(2\lambda_c + \lambda_d)} d\Delta T \quad (3)$$

The force is proportional to the temperature gradient and the forth power of the droplet size. Fig. 7 depicts the manipulation force F_M under typical parameters in our experimental condition, and the magnitude of the force is approximately 1 nN. In comparison with other droplet manipulation method i.e., optical tweezers (Kuo et al, 1993), the photothermal Marangoni technique in the present study can provide the manipulation force 1000 times stronger than that of the optical tweezers.

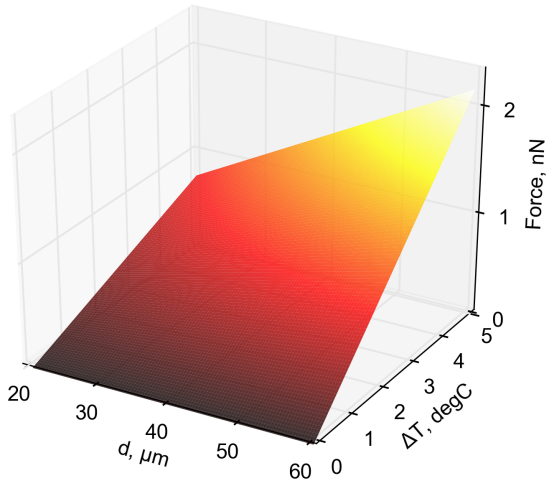

Figure 7: Manipulation force by photothermal Marangoni effect.

3.3.1 Validation force estimation

The manipulation force evaluation was verified by suspending a single droplet with laser heating downstream of it as in Fig. 8. In the situation, the manipulation force F_M by Marangoni convection is balanced against the drag force F_D acting on the droplet. Here, we defined an experimental manipulation force anew as F_{trap}, calculated in Eq. (2) with droplet migration velocity U_M measured upstream of the laser heating area.

Fig. 9 shows comparison of manipulation force between F_M and F_{trap}. The forces obtained by different methods show a good agreement, thus it can be said that our model to determine the manipulation force is valid. The slight difference of the slope would be caused by an assumption of constant temperature gradient around the droplet or temperature-dependent properties.

3.3.2 Manipulation force profile under temperature field

The manipulation force distribution exerting on a droplet with 30 μm diameter under laser-heated temperature field was estimated using Eq. (3). Fig. 10 shows the manipulation force profile on the center section of the heating area in Fig. 6. Here, the direction of the force was based on the flow direction; positive force corresponds streamwise direction.

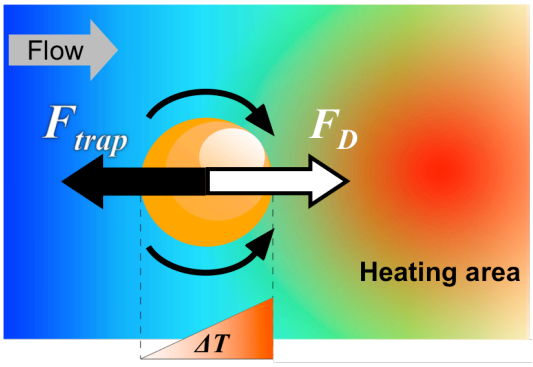

Figure 8: Schematic of force balance on a suspending single droplet by laser heating.

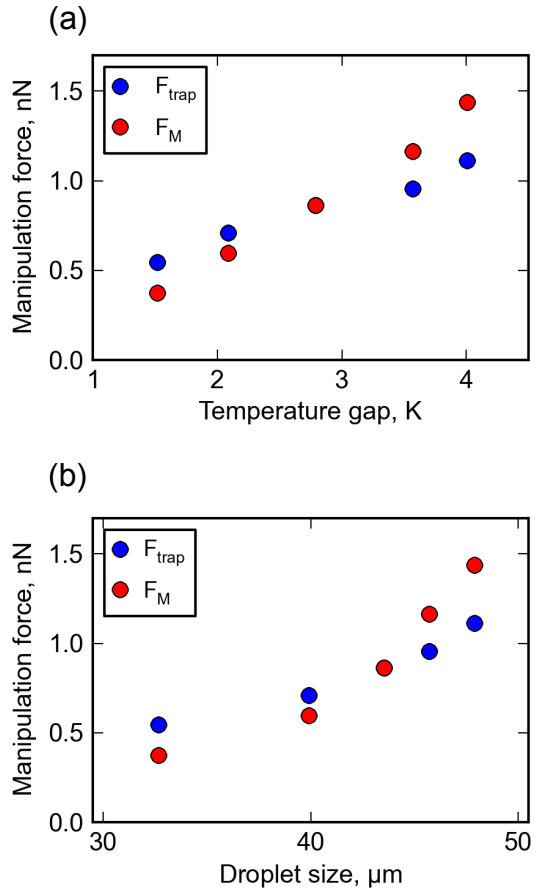

Figure 9: Comparison of manipulation force as a function of (a) temperature gap and (b) droplet size.

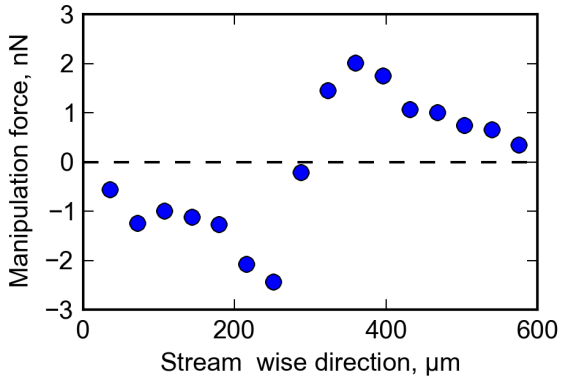

Figure 10: Estimated force profile under temperature field in Figure 6.

As the droplet approaches the center of the heating area (x = 300 μm), the force shows a peak in its magnitude and changes its direction. Based on the proposed model, we can predict the manipulation force exerting on a specific droplet size from the temperature field measured by LIF. The results indicate the potential of the photothermal interfacial activation for practical droplet manipulation using a patterned light illumination.

Acknowlwdgements

The authors thank Specified Research Grant in Tokyo University of Science. A part of microfabrication was performed in Center for Nano Lithography & Analysis, The University of Tokyo, supported by the Ministry of Education, Culture, Sports, Science and Technology (MEXT), Japan. A part of this research was financially supported by Grant-in-Aid for Young Scientists (A) No. 25709013.

References

Baroud, C.N., Delville, J.P., Gallaire, F., 2007, Thermocapillary valve for droplet production and sorting, *Phys. Rev. E* **75**, 046302.

Chen, J., Dagan, Z., Maldarelli, C., 1991, The axisymmetric thermocapillary motion of a fluid particle in a tube, *J. Fluid Mech.* **233**, 405-437.

Kuo, S.C., Sheetz, M.P., 1993, Force of single kinesin molecules measured with optical tweezers, *Science* **260**, 232-234.

Muto, M., Motosuke, M., 2013, On-demand photothermal patterning of pathway for picoliter droplet, *Proc. 17th Int. Conf. Miniaturized Sys. Chem. Life Sci.*, 955-957.

Teh, S.Y, Lin, R., H, L.H, Lee, A.P., 2008, Droplet microfluidics, *Lab Chip* **8**, 198-220.

Xia, Y., and Whitesides, G.M., 1998, Soft lithography, *Annu. Rev. Mater. Sci.* **28**, 153-184.

Young, N.O., Goldstein, J.S., Block, M.J., 1959, The motion of bubbles in a vertical temperature gradient, *J. Fluid Mech.* **6**, 350-356.